Assembly Behavior and Binding Ability of Double-armed Benzo-15-crown-5 with the Potassium Ion

Yu Liu[a]; Jian-Rong Han[a]; Heng-Yi Zhang[a]

[a] Department of Chemistry, State Key Laboratory of Elemento-Organic Chemistry, Nankai University, Tianjin, P. R. China

PLEASE SCROLL DOWN FOR ARTICLE

Assembly Behavior and Binding Ability of Double-armed Benzo-15-crown-5 with the Potassium Ion

YU LIU*, JIAN-RONG HAN and HENG-YI ZHANG

Department of Chemistry, State Key Laboratory of Elemento-Organic Chemistry, Nankai University, Tianjin 300071, P. R. China

Two novel supramolecular aggregations possessing column structures have been prepared from double-armed benzo-15-crown-5 ether (2) and its complex with potassium ion, respectively. Their molecular assembly behavior has been evaluated by calorimetry, ^{1}H NMR, X-ray crystallography and STM images, revealing that the molecular assembly behavior of 2 in the solid state can be controlled by the stepwise sandwiching complexation with the cation.

INTRODUCTION

Crown ethers possessing additional donor atom(s) or other functional group(s) have emerged as one of the most influential architectural motifs for rotaxanes, [1–3] pseudorotaxane, [4–7] daisy chain, [8–13] molecular cables, [14] channels, [15] self-assembled monolayers, [16–19] amphiphilic molecule, [20] nanowires, [21] *etc*. It is noted that hydrogen bonding, π–π stacking interaction, and ion–dipole interaction play a crucial role in the formation of these supramolecular assemblies. Gibson *et al.* [22] described the cooperative self-assembly of dendrimers *via* pseudorotaxane formation from a homotritopic guest molecule and complementary monotopic host dendrons by hydrogen-bonded interaction. Nolte *et al.* [23] reported a self-assembly of disk-shaped molecules to coiled-coil aggregates with tunable helicity by attractive π–π interactions occurring between the aromatic rings. Different from the above π–π stacking, Stoddart *et al.* [8] devised a self-assembling approach to supramolecular polymer formation which relies upon the self-complementarity of monomers incorporating a π-electron rich macrocyclic "head" and a π-electron deficient acyclic "tail" that are unable to interact intramolecularly. Poly(*para*-phenylene vinylene) with crown ether substituents (C-PPV) could form nanoribbons through the interaction between K^+ and crown ether substituents [24]. Unfortunately, there are no comparison studies for the molecular assembly behavior of crown ethers in solution and in the solid state to the best of our knowledge, though it is important to understand the molecular assembly mechanism. In the text, we wish to report our investigation results on the comparison of the self-assembly behavior of crown ether **2** (Scheme 1) and its complex with potassium ion in both solution and the solid state.

EXPERIMENTAL SECTION

General

Melting points, measured with a Xt-4 apparatus, are uncorrected. ^{1}H NMR spectra were recorded on a Varian Mercury VX300 instrument in CDCl$_3$ solution, using tetramethylsilane as an internal reference. Ultraviolet spectra were recorded on Shimadzu UV-2401/PC instruments. Elemental analyses were performed on a Perkin-Elmer 2400C instrument. The Scanning Tunneling Microscope (STM) DS-89S instrument with a W tip, and a sample bias voltage +300 mV, tunneling current 2.10 nA, was used in the scanning tunneling experiment.

*Corresponding author. Fax: +86-22-23503625; +86-22-23504853. E-mail: yuliu@public.tpt.tj.cn
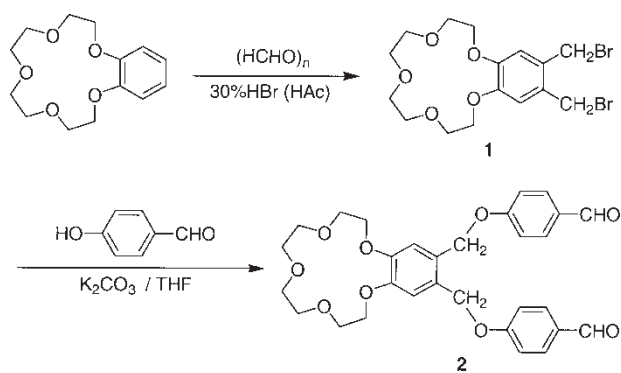
SCHEME 1   Preparation processes of compound **2**.

Materials

Starting materials were commercially available unless noted otherwise. Metal salts (NaCl, KCl) were dried *in vacuo* for 24 h at 120°C prior to use. The methanol was refluxed over magnesium turnings and then distilled. The purified methanol was mixed with distilled, deionized water [$(1.0–1.2) \times 10^{-6}$ S/cm] to make a mixed solvent (8:2/V:V) for calorimetry. The key intermediates 2,3-benzo-1,4,7, 10,13-pentaoxa-2-cyclopentadecene and 2,3-[4′,5′-bis(bromomethyl)-benzo]-1,4,7, 10,13-pentaoxa-2-cyclopentadecene **1** were prepared according to the literature procedure [25,26].

Synthesis 2,3-[4′,5′-Bis[[(4-formoylphenyl)oxy] methyl]-benzo]-1,4,7,10,13-pentaoxa-2-cyclopentadecene (2)

4-Hydroxybenzaldehyde (0.49 g, 4 mmol), anhydrous K_2CO_3 (0.55 g, 4 mmol) and THF (50 ml) were added to a 100 ml reaction flask, which was fitted with magnetic stirrer, reflux condenser and nitrogen gas inlet. After the mixture had been stirred magnetically for 10 min in an inert atmosphere of dry nitrogen, **1** (0.91 g, 2 mmol) was added to the reaction flask, and then the mixture was refluxed for 9 h. After cooling, the solvents were removed *in vacuo*. The residue obtained was added to a mixture of water (100 ml) and chloroform (60 ml), the resultant binary mixture was vigorously stirred, and the chloroform layer was separated and dried over $MgSO_4$. The residue obtained upon evaporation of the chloroform was recrystallized from acetone to give white crystals of **2** (0.88 g, 82%): mp 156–158°C; the crystal structures was revealed by X-ray crystallography. UV–Vis λ_{max}(CHCl$_3$)/nm (ϵ/M^{-1}cm^{-1}) 277.6 (49600), 284.4 (50200); ^{1}H NMR δ 3.76 (d, $J = 3.3$ Hz, 8H), 3.92 (dd, $J_1 = 4.2$ Hz, $J_2 = 3.3$ Hz, 4H), 4.16 (dd, $J_1 = 4.2$ Hz, $J_2 = 3.3$ Hz, 4H), 5.15 (s, 4H), 7.03 (t, 6H), 7.82 (t, 4H), 9.89 (s, 2H). Anal. Calcd for $C_{30}H_{32}O_9$: C, 67.15; H, 6.01. Found: C, 66.89 H, 6.08.
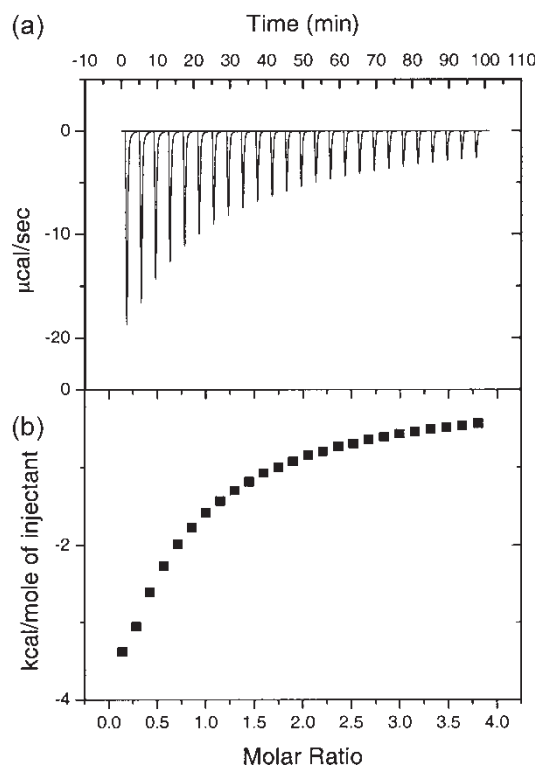

FIGURE 1   Typical calorimetric titration showing binding of K$^+$ to host 2 at 25°C in methanol–water (8:2/V:V). (a) Raw data for sequential 10 µl injections of KCl (20.3 mM) into host 2 (1.02 mM; ITC cell volume 1.4227 ml) and (b) heats of reaction as obtained from the integration of the calorimetric traces.

2–KI Complex

A 10 ml acetone solution of **2** (53.7 mg, 0.1 mmol) and 10 ml methanol solution of KI (8.8 mg, 0.05 mmol) were mixed and stirred at room temperature for overnight. After filtering, the solvent was slowly evaporated at room temperature to afford the complex crystals for X-ray crystallography.

ISOTHERMAL TITRATION

An isothermal calorimeter (VP-ITC), purchased from Microcal, LLC, Northampton MA, was used for all microcalorimetric experiments. The reliability of the whole system and the calculation procedures were doubly checked by comparison of the obtained thermodynamic data of the complexation reaction of β-cyclodextrin with cyclohexanol [27] and benzo-15-crown-5 with Na$^+$, which were shown to be in good agreement with the literature data [28–30]. The microcalorimetric titrations were performed at atmospheric pressure and 25°C in methanol–water solution (8:2/V:V). All solutions were degassed and thermostatted using a Thermo-Vac accessory before titration experiment. In each run, the 0.250 cm^3 syringe containing a solution of the metal ion (20–40 mmol dm^{-3}) was injected into

TABLE I   Crystal data and data collection parameters for **2**-KI and **2**

Data	**2**-KI	**2**
Empirical formula	$C_{61} H_{67} I K O_{19}$	$C_{30} H_{32} O_9$
Formula weight	1270.15	536.56
T (K)	273(2)	293(2)
Crystal system, space group	Monoclinic, $P2_1/c$	Triclinic, P-1
	a = 13.586(8) Å	a = 10.245(3) Å
	b = 30.360(16) Å	b = 11.124(4) Å
	c = 15.894(9) Å	c = 12.367(4) Å
Unit cell dimensions	$\alpha = 90°$	$\alpha = 88.171(7)°$
	$\beta = 113.516(10)°$	$\beta = 85.853(7)°$
	$\gamma = 90°$	$\gamma = 74.120(7)°$
V (Å^3)	6012(6)	1352.0(8) A^3
Z	4,	2,
D_c(mg m^{-3})	1.403	1.318
$F(000)$	2628	568
Crystal size (mm)	$0.30 \times 0.25 \times 0.10$	$0.30 \times 0.25 \times 0.20$
range for data collection	1.34 to 25.03°	2.50 to 25.35°
Data/restraints/parameters	10609/0/741	4780/16/361
Reflections collected/unique	21306/10609 [R (int) = 0.1004]	5620/4780 [R (int) = 0.0241]
Goodness-of-fit on F^2	0.942	1.002
R ($wR2$)[$I > 2\sigma$ (I)]	0.0710 (0.1491)	0.0683 (0.1555)
R ($wR2$) (all data)	0.2006(0.1950)	0.1667 (0.1883)
Largest diff. peak and hole e-A^{-3}	0.866, -0.862	0.499, -0.211

CCDC reference numbers 201535 (**2**) and 201536 (**2**-KI).

the 1.4227 cm^3 stirred (300 rpm) sample cell containing crown ethers solution (1–2.03 mmol dm^{-3}) in methanol–water. Each titration experiment contained 25 successful injections (10 μl per injection). A typical titration curve is shown as Fig. 1. The entire experiment, including automated titration and data acquisition, took place under computer control.

The control experiment in each run was performed to determine the dilution heat of guest in the methanol–water (8:2/V:V) solution without any crown ether present using the same number of injections and concentration of guest as used in the titration experiment. The dilution enthalpy measured in the control experiment was subtracted from the enthalpy determined in the titration experiment for data analysis.
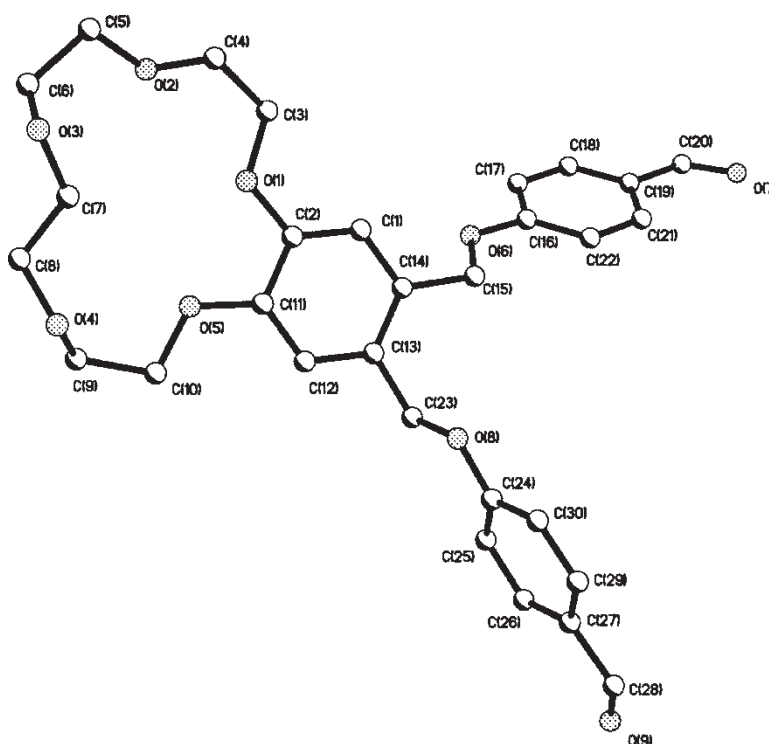

FIGURE 2   X-Ray crystal structure of the crown ether **2**. There is disorder at the O3 site (with fixed 0.75 occupancy) and O3′ with fixed 0.25 occupancy).
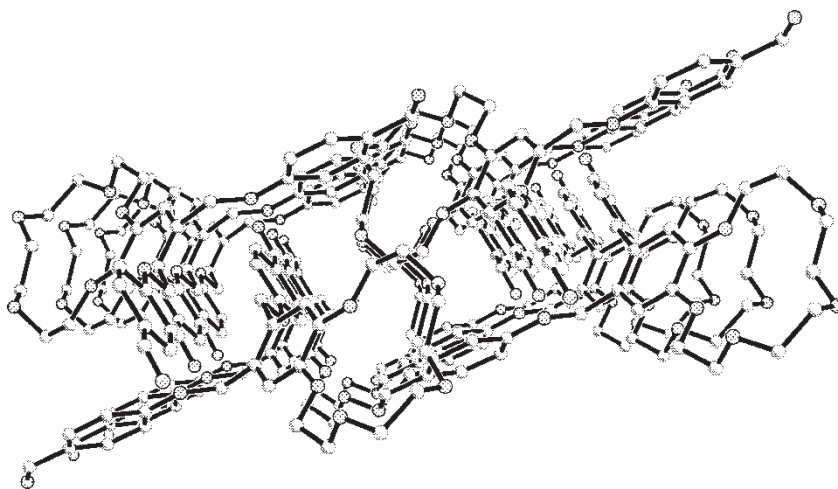
FIGURE 3   Column structure of **2** viewed along the *c* axis.

The ORIGIN software for ITC (version 5, Microcal Inc. Northampton computer program USA) was used to calculate simultaneously the binding constant (K_S) and the enthalpy (ΔH°) of reaction in a single titration experiment. All thermodynamic parameters in this work were obtained in the case of the one set of sites model and two steps sequential binding sites model, with a standard derivation based on the scatter of the data points in a single titration curve simultaneously. Several independent titration experiments were performed to examine the accuracy of these calculated parameters, and

FIGURE 4   X-Ray crystal structure of **2**–K$^+$. Solvent methanol and iodine have been omitted for clarity.

the results and uncertainties given in this text were calculated as weighted averages of the results of the two or three titration experiments.

X-RAY CRYSTALLOGRAPHIC STUDY

The X-ray intensity data of **2** and **2**–KI were collected on a standard Siemens SMART CCD Area Detector System equipped with a normal-focus molybdenum-target X-ray tube ($\lambda = 0.71073\,$Å) operated at 2.0 kW (50 kV, 40 mA) and a graphite monchromator. Crystallographic data for compounds **2** and **2**–KI are summarized in Table I. The structure was solved by using a direct method and refined employing full-matrix least squares on F^2 (Siemens, SHELXTL, version 5.04). CCDC reference numbers 201535 (**2**) and 201536 (**2**–KI)

RESULTS AND DISCUSSION

Description of Crystal Structures

In the crystal **2**, the dihedral angle of the two side-chains is 100.4°, and the adjacent molecules by face-to-face stacking between the side-chain aromatic rings along the *c* axis generate two-dimensional extend layers (Figs. 2 and 3). The centroid–centroid distance of these aromatic groups can be used to rationalize whether a favourable π–π interactions exists [31]. The centroid–centroid distances between the two side-chain aromatic rings in the adjacent molecules are 1.48 Å and 4.00 Å, respectively. There-fore such favourable π–π interactions contribute greatly to the formation of the columnar-structural molecular aggregation.

It is well known that larger cations in size than the crown ether's cavity can form 1:2 (cation:ligand) sandwich complexes in both solution and
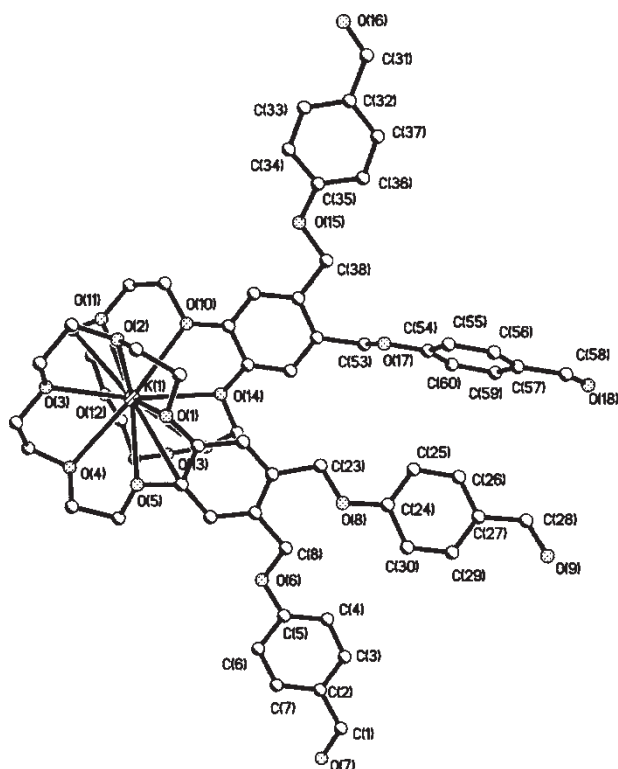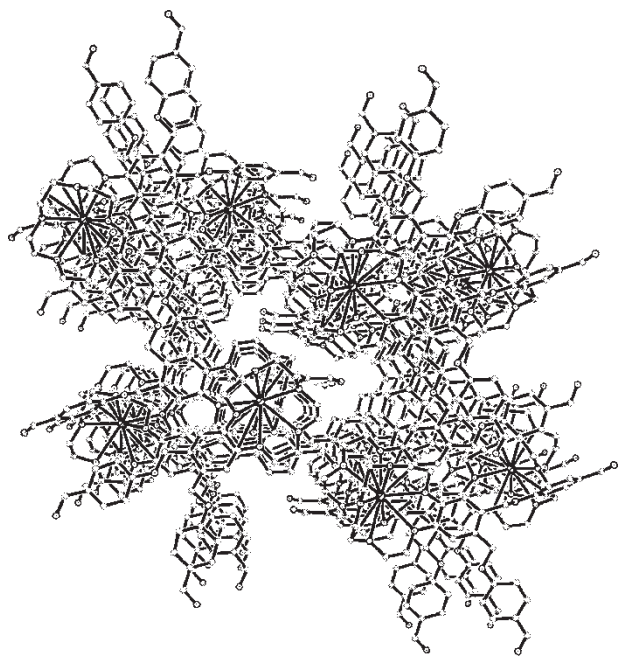
FIGURE 5   Column structure of **2**-KI complex viewed along the *c* axis.

the crystalline state [32–34]. In the crystal **2**–KI, the metal cation is held between a pair of 15-crown-5 rings to form a sandwich structure, in which the distance and the dihedral angle between the two crown rings are 4.31 Å and 2.1°, respectively (Fig. 4). One of the two aromatic rings in the side chains of

2-KI interacts with one of another molecule by $\pi-\pi$ stacking (T shape) [31] with a centroid distance of 4.79 Å and dihedral angle of 81°. In contrast to the crystal structure of the benzo-15-crown-5-K^+ sandwich complex [35], two benzene rings of the benzo-15-crown-5 in the sandwich complex were located on the identical side face of K^+, so as to give rise to favourable $\pi-\pi$ interaction between the two aromatic rings almost parallel at a 3.56 Å average distance. Therefore, substituent effects of **2** could not only alter the original structure of the sandwich complex, but also increase the sandwich complexation stability through $\pi-\pi$ interactions, leading to the formation of a line-knotted supramolecule, as shown in Fig. 5. The distance between the "knots" in the same line is 11.9 Å. We can also see a lot of columnar structures, in which K^+ is filled with a K^+-K^+ distance of 13.6 Å.

^{1}H NMR Spectra

It is not sufficient to elucidate the binding modes in solution by crystal structures. In order to obtain detailed information about the solution structure of the resulting complexes of **2** with cations, ^{1}H NMR spectra of **2**–$CDCl_3$ solutions were measured in the presence and absence of metal ions. The peaks assigned to almost all protons in **2** as depicted in Fig. 6 completely reverse in the presence and absence of Na^+ and K^+. For the resulting complex

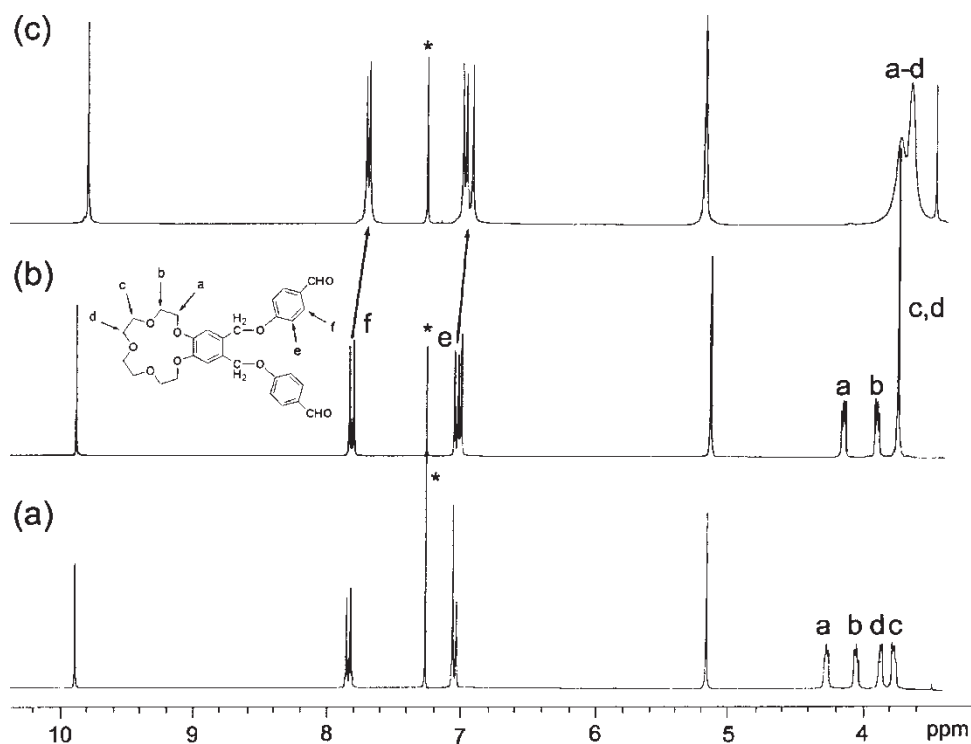FIGURE 6 ^{1}H NMR spectra of (a) **2** in the presence of NaI, (b) free **2** and (c) **2** in the presence of KI, in $CDCl_3$. The peaks labeled with an asterisk are attributed to the solvent.
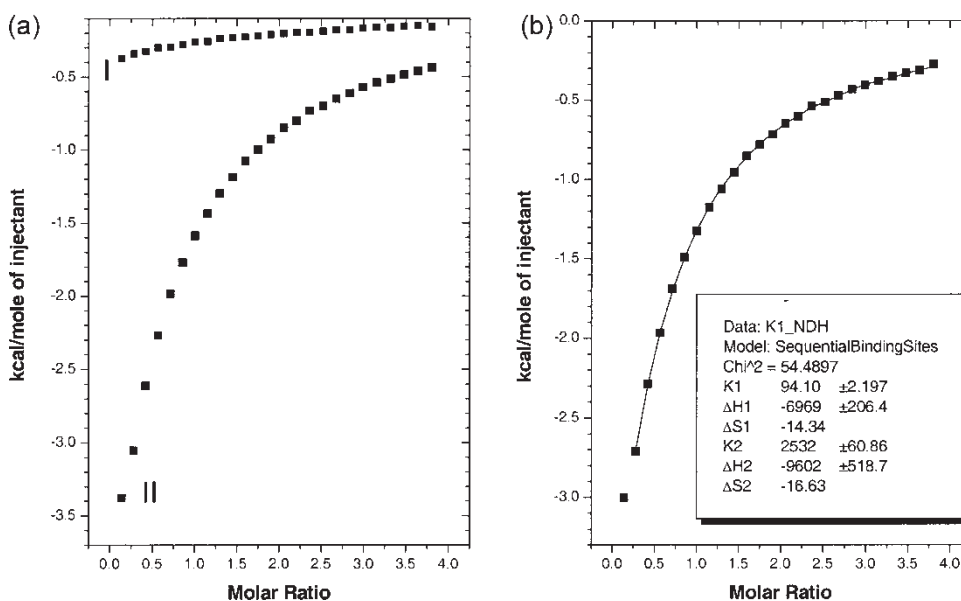
FIGURE 7 (a) Heat effects of the dilution (I) and of the complexation reactions (II) of K^+ and crown ether **2** for each injection during titration microcalorimetric experiments at 298 K; (b) "Net" heat effects of complexation of **2** with K^+ for injection, obtained by subtracting the heat of dilution from the heat of reaction, both of which are fitted to the theoretical curve by computer simulation using the two step sequential binding sites model.

of **2** and Na^+, the chemical shifts of crown ether ring protons shift downfield, and the original single peak of methylene protons in c and d split into two peaks. Apparently, Na^+ matches the cavity of benzo-15-crown-5 in **2** well and thus is just accommodated in the crown ether ring to form 1:1 cation/ligand complexes. The positive charge of Na^+ makes the electron cloud of oxygen atoms lean to the center of the ring, and furthermore, the deformed oxygen electron cloud further induces those electrons around methylene carbons to deflect from hydrogen atoms, resulting in hydrogen protons deshielded by *ca.* 0.01, 0.1, 0.094 and 0.097 ppm relative to their counterparts. These different deshielding effects must be attributed to the difference in the distances between Na^+ and the five oxygen atoms of benzo-15-crown-5 [36], because of the longer distance resulting in the smaller deshielding effect. Differing entirely from the complex **2**–NaI, not only the chemical shifts of crown ether ring protons in **2**–KI complexes shift upfield, but also all the methylene proton peaks are contracted to a broad peak. Reasonable explanations for the chemical shifts are the steric-contract and/or aromatic ring shielding effect of **2** upon complexation with K^+ to form 1:2 cation/ligand sandwich complexes, and the difference in peak shape between the Na^+ and the K^+ complexes is related to the rate of exchange between the bound and the free ligand (slow for Na^+ and intermediate for K^+). Therefore, the formation of the linear polymer supramolecules of **2**–KI in the solid state is a natural process.

Calorimetry

Isothermal titration calorimetry (ITC) was utilized to investigate the thermodynamics of association between crown ether **2** and Na^+ and K^+. The results obtained indicate that the one set of sites model is fit for only the complexation between **2** and Na^+ and two steps sequential binding sites model for the complexation between **2** and K^+, which are consistent with the binding process investigated by ^1H NMR spectra. A typical calorimetric titration curve of host **2** with K^+ is shown in Fig. 7. For the first step reaction of **2** with K^+, its stability constant ($98\,M^{-1}$, averages of the results of the three titration experiments) is in accordance with that between **2** and Na^+ ($96\,M^{-1}$), regardless of a larger entropy loss ($-T\Delta S_1° = 17.39\,kJ\,mol^{-1}$ for **2**/K^+, $-T\Delta S° = 10.49\,kJ\,mol^{-1}$ for **2**/Na^+), One reasonable explanation for this phenomenon is that, K^+ is somewhat too large to fit comfortably and centrosymmetrically within the cavity of 15-crown-5 and is therefore much more likely to adopt "sunrise" conformations, resulting in the larger entropy loss. The larger stability constant ($2512\,M^{-1}$) together with the more negative enthalpic gain ($-\Delta H_2° = 41.72\,kJ\,mol^{-1}$) and the larger entropy loss ($-T\Delta S_2° = 22.36\,kJ\,mol^{-1}$) for the second step reaction between **2** and K^+ means that it is easier to form the sandwich structure. Therefore, the present investigation about the stability and thermodynamic parameters of complexation in solution rationalizes thermodynamically the mechanism of the formation of the linear polymer supramolecules from solution to solid, and on the other hand helps with understanding
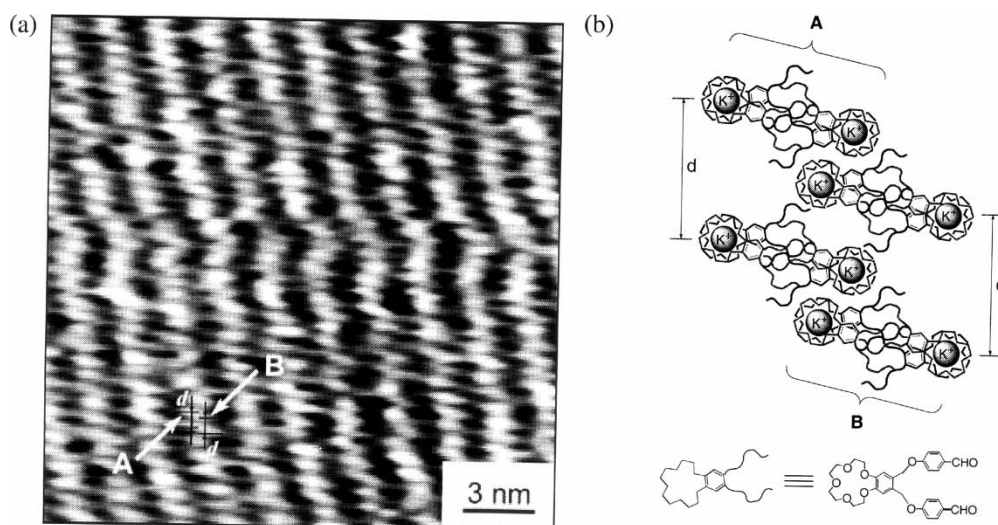
FIGURE 8 (a) STM images of the linear supramolecular aggregates and (b) a proposed structural model for the ordered array of compound **2** and KI.

the thermodynamic origin in the process of the molecular assembly.

STM Image of 2–KI

It is noted that the linear polymer supramolecule could also be observed directly by STM images. A typical STM image can be obtained by dripping a chloroform solution of **2**–KI complexes onto a fresh highly ordered pyrolytic graphite (HOPG). As can be seen from Fig. 8(a), many lines exist on the substrate. Each "bright dot" in fact consists of white dot A and white dot B. According to the size and shape, the length of each white dot (A or B) is *ca.* 0.8–1.2 nm, which is consistent with the width of "knot" in the **2**–KI crystal. Therefore, one may presume reasonably that a white dot A or B is composed of a pair of sandwich complex **2**–KI in the "tail to tail" mode lying on the surface of HOPG. The apparent "bright dot" further formed the linear aggregations with 0.7–1.0 nm distance (*d*) between two adjacent white dots A or white dots B as illustrated in Fig. 8(b), which is less than the distance of two "knots" in the crystal. An explanation for the formation of long, but anomalous contracted linear aggregations can be provided by the above ^{1}H NMR spectrum. The deshielding effect for the aromatic ring proton in side chains of **2** upon complexation with K^+ suggests that there exists a $\pi-\pi$ interaction between these aromatic rings. When the solvent chloroform was removed quickly from the HOPG, the sandwich complex **2**–KI cannot array subtly as the complex does in crystals, and therefore, the shorter distance between the aromatic rings would explain the stronger $\pi-\pi$ interaction, resulting in

the formation of the irregular linear aggregations on the HOPG.

CONCLUSION

In summary, we have presented a columnar structure linear polymeric supramolecule formed by crown ether **2** and KI in the solid state, and demonstrated its formation mechanism by NMR and ITC. The STM experiment provided an insight into the linear polymeric supramolecule on the HOPG. The binding constants and the thermo-dynamic parameters obtained in this study not only reveal the stability of aggregation in solution, but also help to understand the thermodynamic origin in the process of the molecular assembly. Consequently, the systemic investigation provides an example of how to design versatile building units for supra-molecular self-assembly.

References

[1] Dvornikovs, V.; House, B. E.; Kaetzel, M.; Dedman, J. R.; Smithrud, D. B. *J. Am. Chem. Soc.* **2003**, *125*, 8290.
[2] Smukste, I.; Smithrud, D. B. *J. Org. Chem.* **2003**, *68*, 2547.
[3] Smukste, I.; House, B. E.; Smithrud, D. B. *J. Org. Chem.* **2003**, *68*, 2559.

[4] Fitzmaurice, D.; Rao, S. N.; Preece, J. A.; Stoddart, J. F.; Wenger, S.; Zaccheroni, N. *Angew. Chem. Int. Ed.* **1999**, *38*, 1147.

[5] Ryan, D.; Rao, S. N.; Rensmo, H.; Fitzmaurice, D.; Preece, J. A.; Wenger, S.; Stoddart, J. F.; Zaccheroni, N. *J. Am. Chem. Soc.* **2000**, *122*, 6252.

[6] Balzani, V.; Ceroni, P.; Credi, A.; Gómez-López, M.; Hamers, C.; Stoddart, J. F.; Wolf, R. *New J. Chem.* **2001**, *25*, 25.

[7] Gong, C.; Gibson, H. W. *Angew. Chem. Int. Ed.* **1998**, *37*, 310.

[8] Ashton, P. R.; Baxter, I.; Cantrill, S. J.; Fyfe, M. C. T.; Glink, P. T.; Stoddart, J. F.; White, A. J. P.; Williams, J. D. *Angew. Chem. Int. Ed.* **1998**, *37*, 1294.

[9] Ashton, P. R.; Parsons, I. W.; Raymo, F. M.; Stoddart, J. F.; White, A. J. P.; Williams, D. J.; Wolf, R. *Angew. Chem. Int. Ed.* **1998**, *37*, 1913.

[10] Chiu, S. H.; Rowan, S. J.; Cantrill, S. J.; Stoddart, J. F.; White, A. J. P.; Williams, D. J. *Chem. Commun.* **2002**, 2948.

[11] Cantrill, S. J.; Youn, G. J.; Stoddart, J. F. *J. Org. Chem.* **2001**, *66*, 6857.

[12] Rowan, S. J.; Cantrill, S. J.; Stoddart, J. F.; White, A. J. P.; Williams, D. J. *Org. Lett.* **2000**, *2*, 759.

[13] Rowan, S. J.; Stoddart, J. F. *Polym. Adv. Technol.* **2002**, *13*, 777.

[14] Ballardini, R.; Balzani, V.; Clemente-León, M.; Credi, A.; Gandolfi, M. T.; Ishow, E.; Perkins, J.; Stoddart, J. F.; Tseng, H. R.; Wenger, S. *J. Am. Chem. Soc.* **2002**, *124*, 12786.

[15] Beginn, U.; Zipp, G.; Mourran, A.; Walther, P.; Möller, M. *Adv. Mater.* **2000**, *12*, 513.

[16] Arias, F.; Godínez, L. A.; Wilson, S. R.; Kaifer, A. E.; Echegoyen, L. *J. Am. Chem. Soc.* **1996**, *118*, 6086.

[17] Miura, Y.; Kimura, S.; Kobayashi, S.; Imanishi, Y.; Umemura J. *Biopolym.* **2000**, *55*, 391.

[18] Miura, Y.; Kimura, S. *Langmuir* **1998**, *14*, 2761.

[19] Herranz, M.Á.; Colonna, B.; Echegoyen, L. *Proc. Natl. Acad. Sci. USA* **2002**, *99*, 5040.

[20] Gebbink, R. J. M. K.; Sandee, A. J.; Peters, F. G. A.; van der Gaast, S. J.; Feiters, M. C.; Nolte, R. J. M. *J. Chem. Soc., Dalton Trans.* **2001**, 3056.

[21] Akutagawa, T.; Ohta, T.; Hasegawa, T.; Nakamura, T.; Christensen, C. A.; Becher, J. *Proc. Natl. Acad. Sci. USA* **2002**, *99*, 5028.

[22] Gibson, H. W.; Yamaguchi, N.; Hamilton, L.; Jones, J. W. *J. Am. Chem. Soc.* **2002**, *124*, 4653.

[23] Engelkamp, H.; Middelbeek, S.; Nolte, R. J. M. *Science* **1999**, *284*, 785.

[24] Luo, Y.-H.; Liu, H.-W.; Xi, F.; Li, J.; Jin, X. G.; Han, C. C.; Chan, C. M. *J. Am. Chem. Soc.* **2003**, *125*, 6447.

[25] Pedersen, C. J. *J. Am. Chem. Soc.* **1967**, *89*, 2495, 7017.

[26] Luboch, E.; Cygan, A.; Biernat, J. F. *Tetrahedron* **1990**, *46*, 2461.

[27] Liu, Y.; Li, L.; Li, X.-Y.; Zhang, H.-Y.; Wada, T. W.; Inoue, Y. *J. Org. Chem.* **2003**, *68*, 3646.

[28] Rekharsky, M. V.; Inoue, Y. *J. Am. Chem. Soc.* **2002**, *124*, 813.

[29] Rekharsky, M. V.; Schwarz, F. P.; Tewari, Y. B.; Goldberg, R. N.; Tanaka, M.; Yamashoji, Y. *J. Phys. Chem.* **1994**, *98*, 4098.

[30] Izatt, R. M.; Terry, R. E.; Nelson, D. P.; Chan, Y.; Eatough, D. G.; Bradshaw, J. S.; Hansen, L. D.; Christensen, J. J. *J. Am. Chem. Soc.* **1976**, *98*, 7626.

[31] Hunter, C. *Chem. Soc. Rev.* **1994**, *23*, 101.

[32] Pedersen, C. J. *J. Am. Chem. Soc.* **1970**, *92*, 386.

[33] Hilgenfeld, R.; Saenger, S. In *Host Guest Complex Chemistry*; Vogtle, F., Ed.; Springer: Berlin, 1982; **2**, p 1.

[34] Steed, J. W. *Coord. Chem. Rev.* **2001**, *215*, 171.

[35] Mallinson, P. R.; Truter, M. R. *J. Chem. Soc. Perkin II*, **1972**, 1818.

[36] Bush, M. A.; Truter, M. R. *J. Chem. Soc. Perkin II* **1972**, 341.